23

Paddle Juggling by Robot Manipulator with Visual Servo

Akira Nakashima, Yoshiyasu Sugiyama and Yoshikazu Hayakawa
Nagoya University
Japan

1. Introduction

Juggling is a typical example to represent dexterous tasks of humans. There are many kinds of juggling, e.g., the ball juggling and club juggling in Fig. 1. Other kinds are the toss juggling, bouncing juggling, wall juggling, wall juggling, box juggling, devil sticks, contact juggling and so on. These days, readers can watch movies of these juggling in the website youtube and must be surprised at and admire many amazing dexterous juggling.
The paddle juggling is not major juggling and may be most easy juggling in all kinds of juggling. The paddle juggling means that one hits a ping-pong ball iteratively in the inverse direction of the gravity by a racket as shown in Fig. 2. Most people can easily hit a ball a few times as the left figure since it is easy to hit the ball iteratively. However, most people finally miss out on the juggling as the right figure since it is difficult to control the hitting position. Therefore, realizing the paddle juggling by a robot manipulator is challenging and can lead to solution of human dexterity.
As mentioned previously, the paddle juggling of a ball by a robot manipulator is composed of three parts: the first part is to iterate hitting the ball, the second part is to regulate the incident angle of the ball to the racket, and the third part is to regulate the hitting position and the height of the hit ball. M. Buehler et. al. (Buehler, Koditschek, and Kindlmann 1994) proposed the mirror algorithms for the paddle juggling of one or two balls by a robot having one degree of freedom in two dimensional space, where the robot motion was symmetry of the ball motion with respect to a horizontal plane. This method achieved hitting the ball iteratively. R. Mori et. al. (R. Mori and Miyazaki 2005) proposed a method for the paddle juggling of a ball in three dimensional space by a racket attached to a mobile robot, where the trajectory of the mobile robot was determined based on the elevation angle of the ball. This method achieved hitting the ball iteratively and regulating the incident angle. These algorithms are simple and effective for hitting the ball iteratively. However, their method does not control the hitting position and the height of the ball. On the other hand, S. Schaal et. al. (Schaal and Atkeson 1993) proposed a open loop algorithm for one-dimensional paddle juggling of one ball. S Majima et. al. (Majima and Chou 2005) proposed a method for the paddle juggling of one ball with the receding horizon control base on the impulse information of the hit ball. Their methods achieved regulating the height of the ball. However, the control problem is only considered in one dimensional space. This study propose a method to achieve paddle juggling of one ball by a racket attached to a robot

manipulator with two visual camera sensors. The method achieve hitting the ball iteratively and regulating the incident angle and the hitting position of the ball. Furthermore, the method has the robustness against unexpected disturbances for the ball. The proposed method is composed of juggling preservation problem and ball regulation problem. The juggling maintenance problem means going on hitting the ball iteratively. The ball regulation problem means regulating the position and orientation of the hit ball. The juggling preservation problem is achieved by the tracking control of the racket position for a symmetry trajectory of the ball with respect to a horizontal plane. This is given by simply extending the mirror algorithm proposed in (Buehler, Koditschek, and Kindlmann 1994). The ball regulation problem is achieved by controlling the racket orientation, which is determined based on a discrete transition equation of the ball motion. The effectiveness of the proposed method is shown by an experimental result.

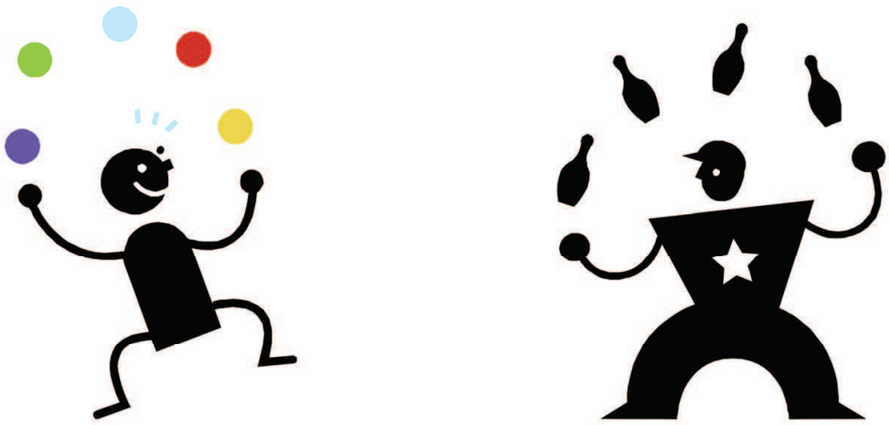

Figure 1. Examples of Juggling: Ball Juggling and Club Juggling

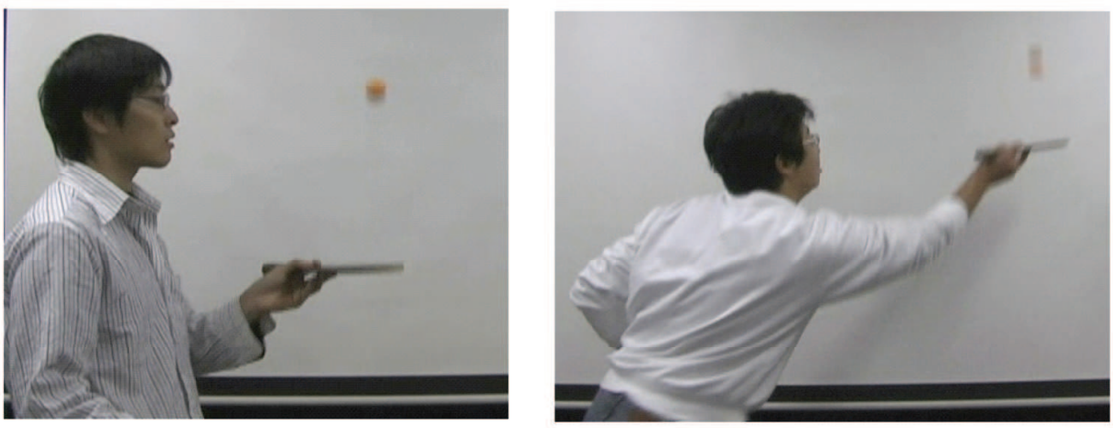

Figure 2. Paddle Juggling: Stable and Unstable Juggling

Section 2 shows the experimental equipments. In Section 3, the system configuration and the models of the manipulator and the ball motion are shown. As for the preliminary of the paddle juggling, the manipulator dynamics are linearized in Section 4. In Section 5, the control designs for the juggling preservation and the ball regulation problems are shown.

An experimental result is shown in Section 6 and the conclusion in this paper and our further Manipulator, works are described in Section 7.

2. Experiment System

We use two CCD cameras and a robot manipulator as shown in Fig. 3 for realizing the paddle juggling. With these equipments, the experiment system is constructed as Fig. 4 composed of a robot manipulator, DOS/V PC as a controller, two CCD cameras, an image processing implement, two image displays and a ping-pong ball. The robot manipulator has 6 joints J_i (i = 1, ... ,6), to which AC servo motors with encoders are attached. The motors are driven by the robot drivers with voltage inputs corresponding the motor torques from the PC through the D/A board. The joint angles are calculated by counting the encoder pluses with the counter board. On the other hand, the image processing implement can detect pixel and calculate the center point of the detected pixel area in two assigned squared areas with thresholds of the brightness. Furthermore, the assigned squared areas can track the calculated center points such that the points are within the areas. The tracked center points are sent to the PC as the image futures. The image data and the image futures can be watched by the two image displays. The cameras are located as the image plane corresponding to the CCD camera include the robot manipulator. Since the ball is very smaller than the robot, the image pixel area of the ball in the image plane has the almost same size as the ball. Therefore, we put the tracking squared areas to the detected pixel of the ball and calculate the position of the ball from the tracked image futures.

The robot is made by DENSO, Inc.. The physical parameters of the robot are shown in Fig 5. J_i and W_i (i = 1, ... ,6) denote the ith joint and the center of mass of the ith link respectively. The values of W_{lr} W_2, W_3, W_4, W_{56} are 6.61, 6.60, 3.80, 2.00 and 2.18 [kg] respectively. The rated torques are 0.25[N-m] (J_1-J_3) and 0.095[N-m] (J_4-J_6). The reduction gear ratios are 241.6, 536, 280, 200, 249.6 and 139.5. The racket is a square plate made from aluminum. The sides, the thickness and the mass are 150, 3[mm] and 0.20[kg] respectively. The ball is a ping-pong ball with the radius and the mass being 35[mm] and 2.50 x 10^{-3}[kg].

The image processing implement is QuickMAG (OKK, Inc.) and the CCD cameras are CS8320 (Tokyo Electronic Equipment, Inc.). The pixel and the focal length of the each camera are 768(H) x 498(W) and 4.8[mm] respectively. The sampling period is 120[Hz]. The PC for the QuickMAG is the FMV-DESK POWER S III 167 (Fujitsu, Inc.). The QuickMAG can track boxed areas to two targets simultaneously and the boxes can be resized easily.

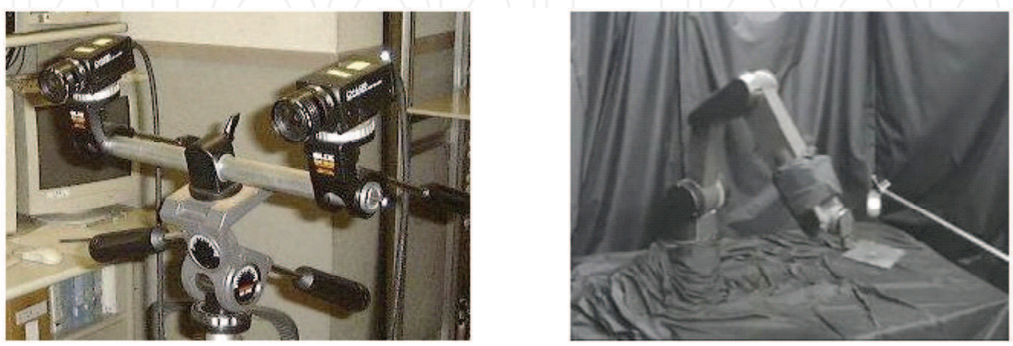

Figure 3. Two CCD cameras and a Robot

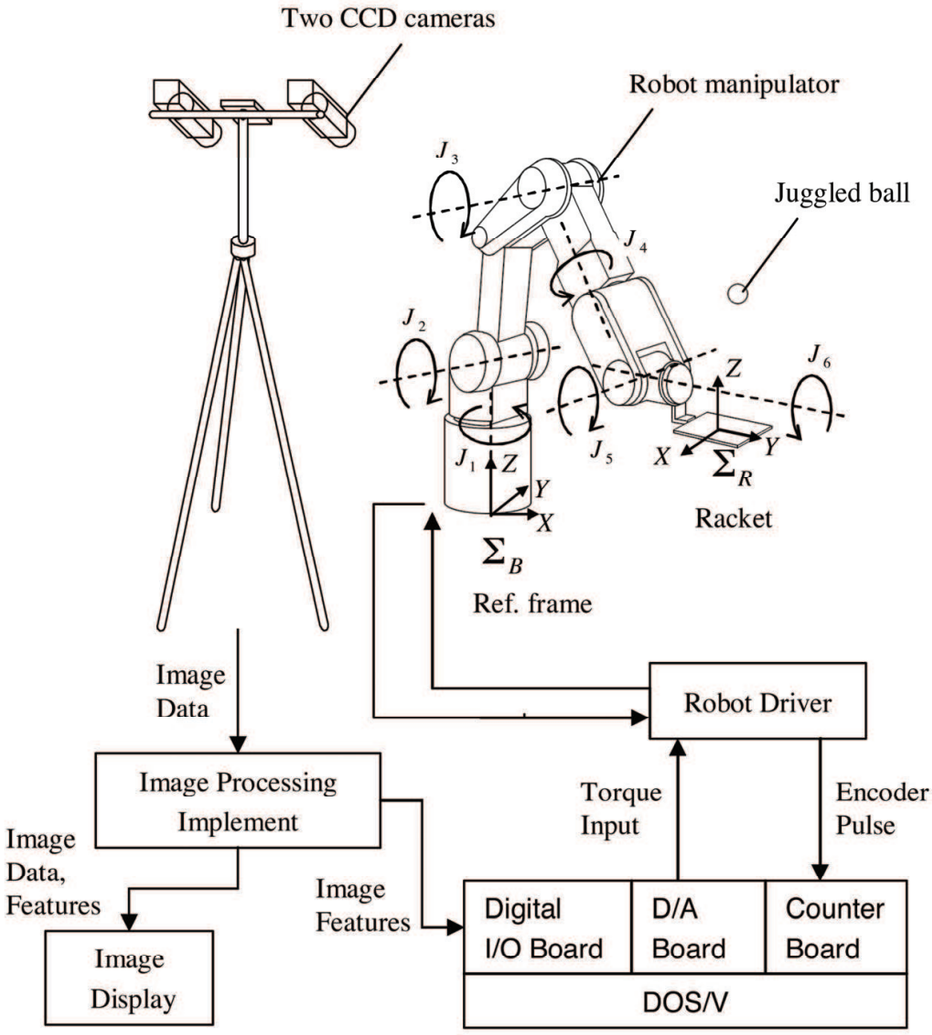

Figure 4. Padde Juggling of a Ball by Camera-Robot System

The PC is the DELL OptiPlex Gxi (CPU:Celeron IGHz, Memory: 256MB). The control method is programmed in C language with Borland C++ 5.5. The D/A board is the DA12-8 (PC) with 12 bit resolution and 9 ch (PC) (CONTEC, Inc.). The counter board is the CNT24-4 (PC) with up-down count in 4 channels (CONTEC, Inc.). The digital board is the IBX-2752C with the 32 number of I/O (Interface, Inc.).

3. Modeling

3.1 System Configuration

In this paper, we consider control of paddle juggling of one ball by a racket attached to a robot manipulator with two-eyes camera as shown in Fig. 4. In this paper, the juggled ball is supposed to be smaller and lighter than the racket. The reference frame Eg is attached at the base of the manipulator. The position and orientation of the racket are represented by the

frame Σ_R, which is attached at the center of the racket. The camera is calibrated with respect to Σ_B. Therefore, the position of the juggled ball can be measured as the center of the ball which the two cameras system detects. (B. K. Ghosh and Tarn 1999). It is obvious that the orientation of the racket about z-axis with respect to Eg does not effect on the ball motion at the time when the racket hits the ball. Therefore we need only 5 degrees of freedom of the manipulator. In the following discussion, the fourth joint J_4 is assumed to be fixed by an appropriate control.

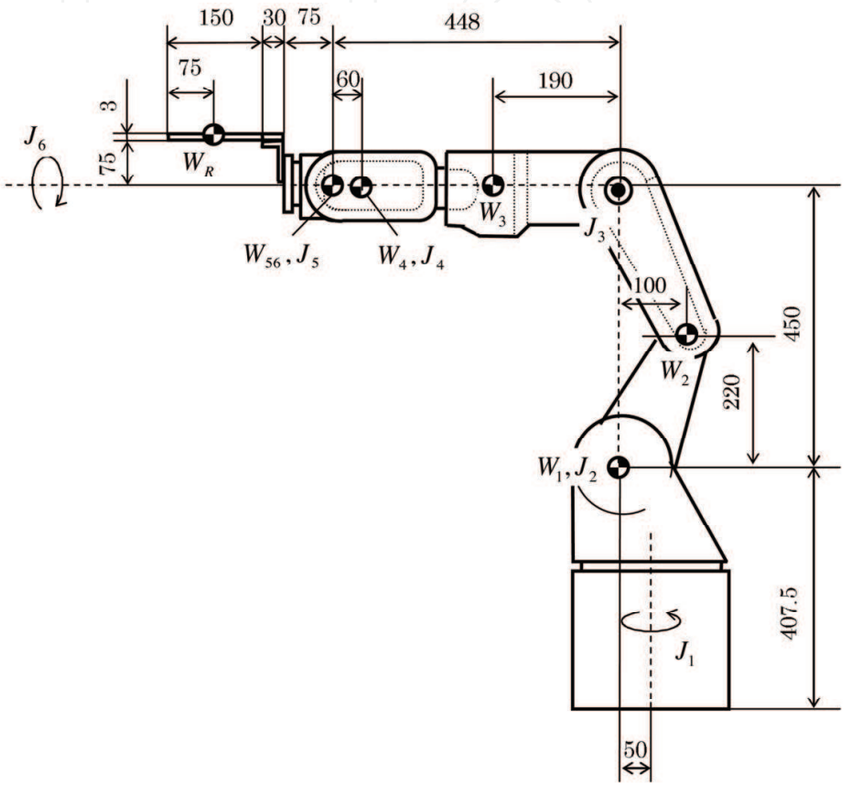

Figure 5. The physical parameters of the manipulator

3.2 Dynamical Equation of Manipulator

The dynamical equation of the manipulator is given by

$$\boldsymbol{M}(\boldsymbol{q})\ddot{\boldsymbol{q}} + \boldsymbol{C}(\boldsymbol{q}, \dot{\boldsymbol{q}})\dot{\boldsymbol{q}} + \boldsymbol{N}(\boldsymbol{q}) = \boldsymbol{\tau}, \tag{1}$$

where $\boldsymbol{q} \in \mathbb{R}^5$ and $\boldsymbol{\tau} \in \mathbb{R}^5$ describe the joint angles and the input torques respectively, and $\boldsymbol{M} \in \mathbb{R}^{5\times5}$, $\boldsymbol{C} \in \mathbb{R}^{5\times5}$ and $\boldsymbol{N} \in \mathbb{R}^5$ are the inertia matrix, the coriolis matrix and the gravity term respectively. For the following discussion, we introduce the following coordinate transformations:

$$^B\boldsymbol{p}_R := \boldsymbol{h}_1(\boldsymbol{q}) \in \mathbb{R}^3, \quad ^B\boldsymbol{\theta}_R := \boldsymbol{h}_2(\boldsymbol{q}) \in \mathbb{R}^2, \tag{2}$$

where $^B\boldsymbol{p}_R = [\ ^Bp_{Rx}\ \ ^Bp_{Ry}\ \ ^Bp_{Rz}\ ]^{\mathrm{T}} \in \mathbb{R}^{3_3}$ is the position of Σ_R with respect to Σ_B, $[\ ^B\theta_{Rx}\ \ ^B\theta_{Ry}\ ]^{\mathrm{T}} \in \mathbb{R}^2$ is the orientation of Σ_R; with respect to x- and y- axes of Σ_B. The left

superscript B of the vector denotes that the vectors are expressed with respect to the frame Σ_B. This notation is utilized for another frames in the following. The functions $\boldsymbol{h}_1(\boldsymbol{q})$ and $\boldsymbol{h}_1(\boldsymbol{q})$ describe the relationships between the position/orientation of the racket and the joint angles respectively. Differentiating (2) with respect to time t and getting together the resultant equations yield the velocity relationship

$$\dot{\boldsymbol{x}}_R = \boldsymbol{J}_R(\boldsymbol{q})\dot{\boldsymbol{q}}, \tag{3}$$

where

$$\begin{aligned} \boldsymbol{J}_R &:= [\,(\partial \boldsymbol{h}_1/\partial \boldsymbol{q})^{\mathrm{T}} \;\; (\partial \boldsymbol{h}_2/\partial \boldsymbol{q})^{\mathrm{T}}\,]^{\mathrm{T}} \in \mathbb{R}^{5\times 5} \\ \boldsymbol{x}_R &:= [\,{}^B\boldsymbol{p}_R^{\mathrm{T}} \;\; {}^B\boldsymbol{\theta}_R^{\mathrm{T}}\,] \in \mathbb{R}^5. \end{aligned}$$

Applying the relationship (3) for the dynamical equation (1) yields the dynamical equation with respect to the position and orientation of the racket

$$\boldsymbol{M}_R(\boldsymbol{q})\ddot{\boldsymbol{x}}_R + \boldsymbol{C}_R(\boldsymbol{q},\dot{\boldsymbol{q}})\dot{\boldsymbol{x}}_R + \boldsymbol{N}_R(\boldsymbol{q}) = \boldsymbol{J}_R(\boldsymbol{q})^{-\mathrm{T}}\boldsymbol{\tau}, \tag{4}$$

where

$$\begin{aligned} \boldsymbol{M}_R &:= \boldsymbol{J}_R^{-\mathrm{T}}\boldsymbol{M}\boldsymbol{J}_R^{-1} \in \mathbb{R}^{5\times 5} \\ \boldsymbol{C}_R &:= \boldsymbol{J}_R^{-\mathrm{T}}\boldsymbol{C}\boldsymbol{J}_R^{-1} + \boldsymbol{J}_R^{-\mathrm{T}}\boldsymbol{M}\tfrac{d}{dt}\boldsymbol{J}_R^{-1} \in \mathbb{R}^{5\times 5} \\ \boldsymbol{N}_R &:= \boldsymbol{J}_R^{-\mathrm{T}}\boldsymbol{N} \in \mathbb{R}^5. \end{aligned}$$

3.3 Equation of Motion and Rebound Phenomenon of Ball

For the modeling of the equation of motion and the rebound phenomenon of the ball, we make the following assumptions:

[Assumption 1] There does not exist the air resistance for the ball.

[Assumption 2] The rebound phenomenon between the ball and the racket is the perfectly elasticity. The surfaces of the ball and the racket are uniform, therefore, the restitution coefficients are isotopic without the incident direction.

[Assumption 3] The mass of the racket is bigger than the mass of the ball such that the racket velocity does not change due to the rebound phenomenon.

Define the ball position by ${}^B\boldsymbol{p}_b := [\,{}^Bp_{bx}\;\; {}^Bp_{by}\;\; {}^Bp_{bz}\,]^{\mathrm{T}} \in \mathbb{R}^3$ From Assumption 1, the equation of motion of the ball is given by

$${}^B\dot{p}_{bx} = v_{b_{xy}}\cos\theta, \;\; {}^B\dot{p}_{by} = v_{b_{xy}}\sin\theta, \tag{5}$$

$${}^B\ddot{p}_{bz} = -mg, \tag{6}$$

where $v_{b_{xy}}$ and θ are the velocity and the direction angle in the (x,y) plane respectively, m[kg] is the mass of the ball and g[m/s^2] is the gravitational constant. Note that (5) represents the ball motion in the (x, y) plane, which is the uniform motion, and $v_{b_{xy}}$ and θ are determined by the motion and the orientation of the racket at the hitting. From Assumption 2 and 3, the mathematical model of the rebound phenomenon is given by

$${}^B\dot{\boldsymbol{p}}_b(t_r + dt) = \boldsymbol{R}_{BR}\boldsymbol{E}\boldsymbol{R}_{BR}^{\mathrm{T}}({}^B\dot{\boldsymbol{p}}_b(t_r) - {}^B\dot{\boldsymbol{p}}_R(t_r)) + {}^B\dot{\boldsymbol{p}}_R(t_r), \tag{7}$$

where t_r is the start time of the collision between the ball and the racket, dt is the time interval of the collision, $\boldsymbol{R}_{BR} \in \mathbb{R}^{3\times3}$ is the rotation matrix from Σ_R to Σ_B and $\boldsymbol{E} := \mathrm{diag}(e_{xy}, e_{xy}, -e_z) \in \mathbb{R}^{3\times3}$ represents the restitution coefficients of the x, y and z directions with respect to Σ_R.

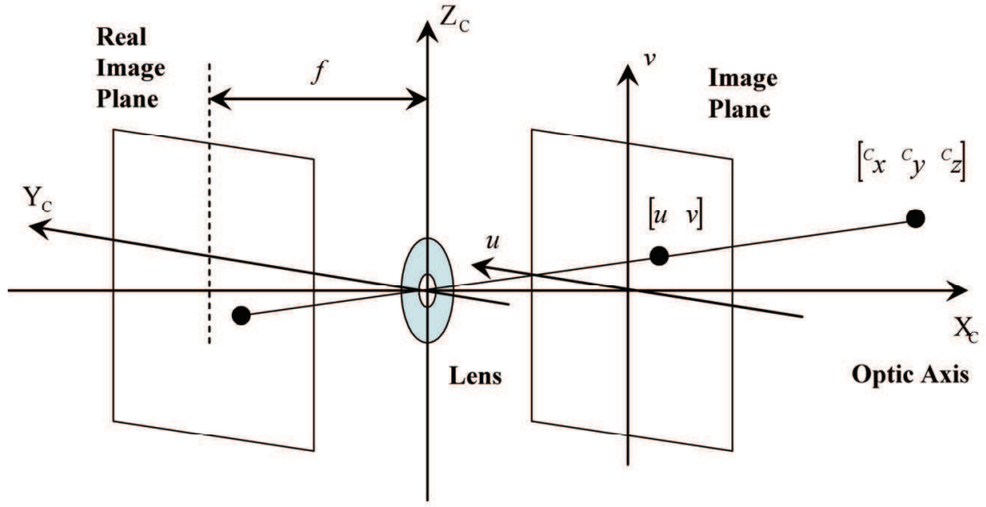

Figure 6. Perspective Transformation Model of Lens

3.4 Perspective Transformation Model of Cameras

Figure 6 shows the perspective transformation of a lens as the pin-hole camera. The camera frame Σ_C is attached the center of the lens and a point p is denoted by a position vector ${}^C\boldsymbol{p} := [{}^Cx\ {}^Cy\ {}^Cz]^{\mathrm{T}} \in \mathbb{R}^3$ expressed in Σ_C. The point p is projected on the real image plane with the focal length f in the inverse direction of the X_C axis. For simplicity, the image feature vector $\boldsymbol{\xi} := [u\ v]^{\mathrm{T}} \in \mathbb{R}^2$ is defined as the coordinates of the projected point on the image plane with the focal length f in the direction of the X_C axis. From the geometric view point, the relationship between the image feature $\boldsymbol{\xi}$ and the position ${}^C\boldsymbol{p}$ is given by

$$\begin{bmatrix} u \\ v \end{bmatrix} = \begin{bmatrix} \dfrac{f}{\alpha_u}\dfrac{{}^Cy}{{}^Cx} \\ \dfrac{f}{\alpha_v}\dfrac{{}^Cz}{{}^Cx} \end{bmatrix}, \tag{8}$$

where α_u and α_v [m/pixel] are the lengths of the unit pixel in the u and v directions. These camera parameters are f = 8.5 x 10~³[m], α_u = 8.4 x 10~⁷ and α_v = 9.8 x 10^⁷ [m/pixel].

4. Linearizing Compensator for Manipulator

As for the preliminary to control the paddle juggling, we linearize the manipulator dynamics (4) by the following linearizing compensator:

$$\boldsymbol{\tau} = \boldsymbol{J}_R^{\mathrm{T}}(\boldsymbol{M}_R\boldsymbol{u}_R + \boldsymbol{C}_R\dot{\boldsymbol{x}}_R + \boldsymbol{N}_R), \tag{9}$$

where $\boldsymbol{u}_R := [\,\boldsymbol{u}_{Rp}^{\mathrm{T}}\ \ \boldsymbol{u}_{R\theta}^{\mathrm{T}}\,]^{\mathrm{T}} \in \mathbb{R}^5$ is the new input for $\ddot{\boldsymbol{x}}_R$. Substituting (9) into (4) results in

$$\boldsymbol{M}_R(\ddot{\boldsymbol{x}}_R - \boldsymbol{u}_R) = \boldsymbol{0}.$$

Since $\boldsymbol{M}_R = \boldsymbol{J}_R^{-\mathrm{T}}\boldsymbol{M}\boldsymbol{J}_R^{-1}$ is the positive definite matrix because the inertia matrix $\boldsymbol{M}$ is positive definite, $\boldsymbol{M}_R$ always has the inverse matrix. Therefore, we get the linearized equations given by

$$^{B}\ddot{\boldsymbol{p}}_R = \boldsymbol{u}_{Rp}, \tag{10}$$

$$^{B}\ddot{\boldsymbol{\theta}}_R = \boldsymbol{u}_{R\theta}. \tag{11}$$

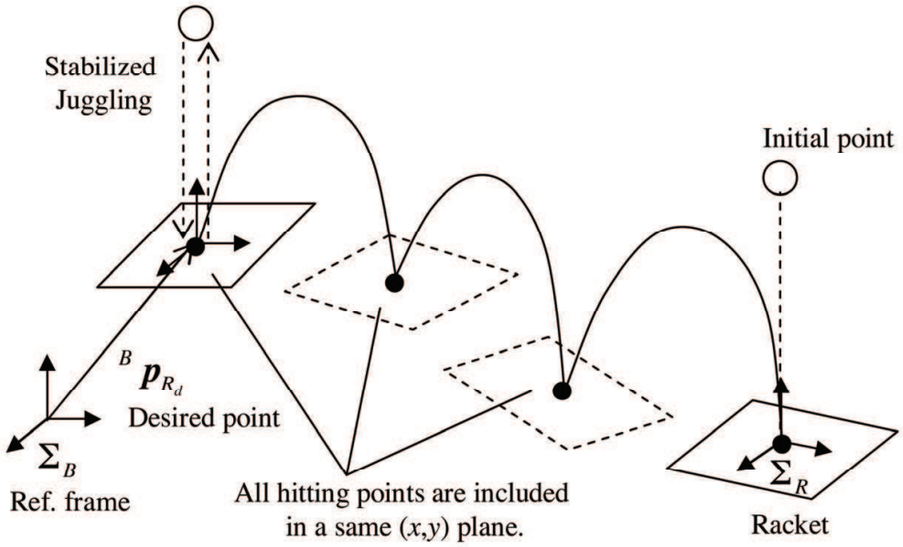

Figure 7. The concept for Padde Juggling of one Ball

The tracking control of $^{B}\boldsymbol{p}_R$ and $^{B}\boldsymbol{\theta}_R$ can be easily realized by PD controller for $\boldsymbol{u}_{Rp}$ and $\boldsymbol{u}_{R\theta}$, for example. In the following discussion, let us consider the desired values of $^{B}\boldsymbol{p}_R$ and $^{B}\boldsymbol{\theta}_R$ to realize the paddle juggling of the ball.

5. Control Design for Paddle Juggling

5.1 Control Objectives

Figure 7 illustrates the control purpose. The initial point of the ball is above the racket and the ball is freely released. The control purpose is to achieve the paddle juggling of the ball at the desired hitting point $^{B}\boldsymbol{p}_{R_d}$ by hitting the ball with the racket iteratively. This is described by the following specific control problems:

1. [Juggling Preservation Problem]
   The juggling maintenance problem means going on hitting the ball iteratively. The control of the ball position is not included in this problem.
2. [Ball Regulation Problem]
   The ball regulation problem means regulating the hitting position of the hit ball. The regulation of the ball height is not included in this problem.

In the following sections, the control designs for these control problems are shown.

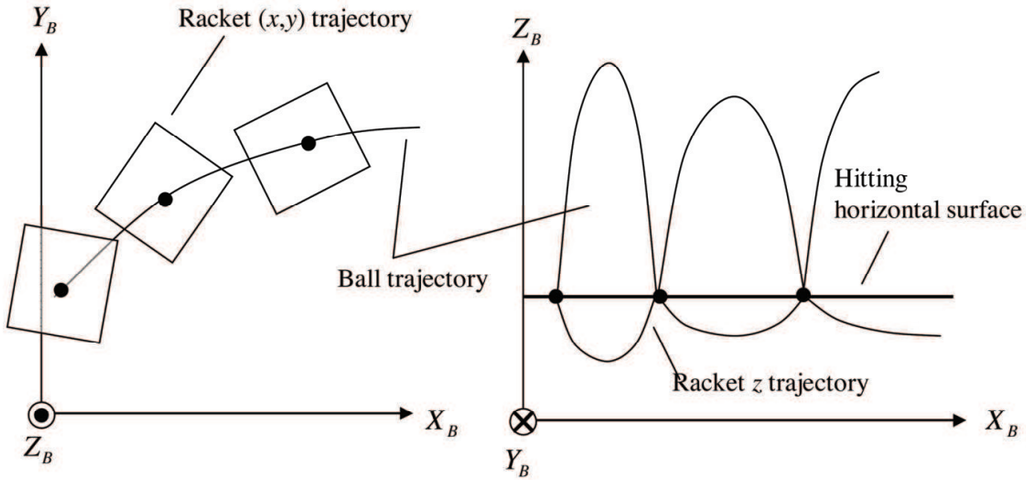

(a) Trajectory of (x,y) (b) Smaller opposite trajectory of z

Figure 8. Control Scheme for the Racket Position Control

5.2 Control Design for Juggling Preservation Problem

The control design for the juggling preservation problem with controlling the racket position ${}^B\boldsymbol{p}_R$ is shown. We firstly consider that the ball is always hit by the racket in a same (x,y) plane as shown in Fig. 7. This plane is called the hitting horizontal plane in this paper. More specific determination of the racket position is shown in Fig. 8. As in the left figure (a), the x and y coordinates of the racket are forced to follow the x and y coordinates of the ball. On the other hand, as in the right figure (b), the z coordinate of the racket is forced to follow the symmetric trajectory of the z coordinate of the ball with respect to the hitting horizontal plane. The desired value of the racket position ${}^B\boldsymbol{p}_{R_d}$ to satisfy the mentioned in the above is given by

$$ {}^B\boldsymbol{p}_{R_d} := \begin{bmatrix} {}^Bp_{b_x} \\ {}^Bp_{b_y} \\ {}^Bp_h - k_h({}^Bp_{b_z} - {}^Bp_h) \end{bmatrix}, \tag{12} $$

where ${}^Bp_h$ is the height of the hitting horizontal plane and $0< k_h <1$ the constant to make the z coordinate of the racket small appropriately. Note that effects on the height of the hitting ball.

Due to determining the desired value of the racket position ${}^B\boldsymbol{p}_R$ by (12), there always exists the racket under the ball and the ball is hit in the same horizontal plane automatically. This determination of the racket position is based on the mirror algorithm (Buehler, Koditschek, and Kindlmann 1994).

5.3 Control Design for Ball Regulation Problem

For preliminary, we introduce a frame based on the states of the ball at the hitting. In Fig. 9 (a), the origin of Σ_H is the hitting position. The Y_H- axis is defined as the direction of the ball motion in the (x,y)-plane at the hitting, and the Z_H- axis is defined as the same direction of Z_B of Σ_B. The X_H- axis is defined such that Σ_H is the right-handed frame. θ_H and θ_R denote

the angles of Y-axes of Σ_H and Σ_R respectively. The relationship between these two frames is represented by the rotation matrix

$$\boldsymbol{R}_{RH} := \begin{bmatrix} \cos(\theta_R - \theta_H) & \sin(\theta_R - \theta_H) \\ -\sin(\theta_R - \theta_H) & \cos(\theta_R - \theta_H) \end{bmatrix}, \tag{13}$$

where

$$\theta_H := \sin^{-1}\left(\frac{\dot{p}_{b_y}}{\sqrt{\dot{p}_{b_x}^2 + \dot{p}_{b_y}^2}}\right). \tag{14}$$

We consider the racket orientation ${}^H\boldsymbol{\theta}_R := [\ {}^H\theta_{R_x}\ \ {}^H\theta_{R_y}\ ]^{\mathrm{T}}$ with respect to Σ_H as shown in Fig. 9 (b).

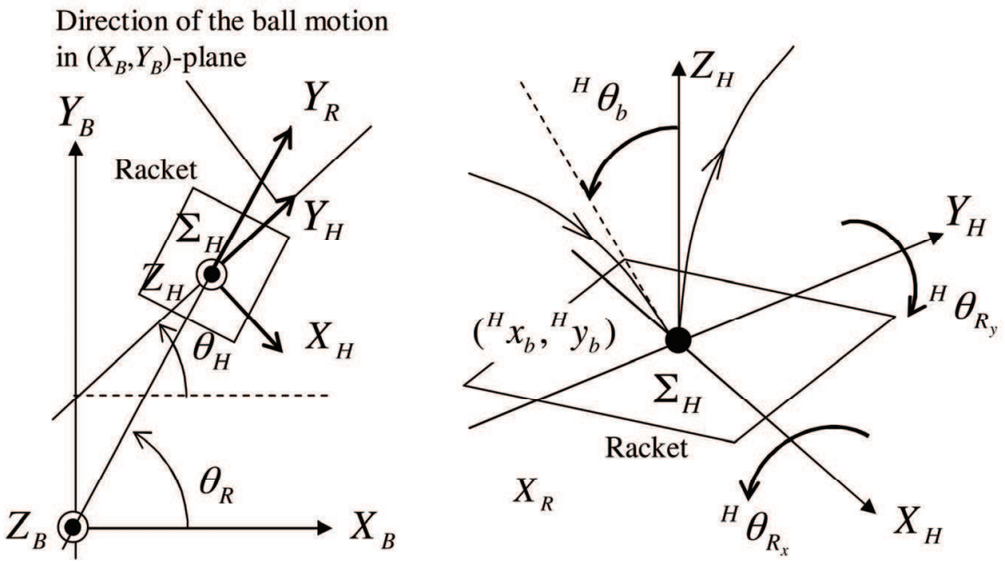

(a) Frame Σ_H defined at hitting (b) Racket orientation w.r.t. Σ_H

Figure 9. Racket Orientation w. r. t. Σ_H Denned by Ball Sates at Hitting

In the frame Σ_H defined above, let us consider the ball regulation problem by the racket orientation ${}^H\boldsymbol{\theta}_R$. For the derivation simplicity of the transition equation of the hit ball, the translational velocity of the racket is assumed to be zero. The control variables are the incidence angle ${}^H\theta_b[i]$ from the Z_H- axis and the position $({}^Hx_b[i], {}^Hy_b[i])$ at the hitting point as shown in Fig. 9 (b). The constant i (i = 0,1,2, ...) represents the number of the hitting. Note that ${}^H\theta_{R_x}$ effects on both $({}^Hy_b, {}^H\theta_b)$, and ${}^H\theta_{R_y}$ effects on only ${}^Hx_b$. Therefore, the ball transition by the hitting can be separated to the Y_H- and X_H- directions illustrated in Fig. 10. The figure (a) shows the transition of the incident angle ${}^H\theta_b$ and the position ${}^Hy_b$, and the figure (b) shows the transition of the position ${}^Hx_b$. From (5)-(7), the relationships between $({}^Hx_b[i], {}^Hy_b[i], {}^H\theta_b[i])$ and $({}^Hx_b[i+1], {}^Hy_b[i+1], {}^H\theta_b[i+1])$ are given by

$${}^Hx_b[i+1] = {}^Hx_b[i] + \frac{(v_{b_0}\cos{}^H\theta_b[i])^2 \sin 4{}^H\theta_{R_y}[i]}{g} \tag{15}$$

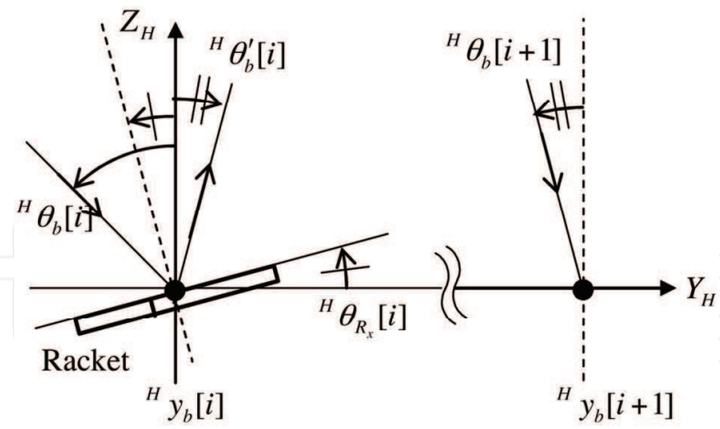

(a) Incident angle and y coordinate of Ball

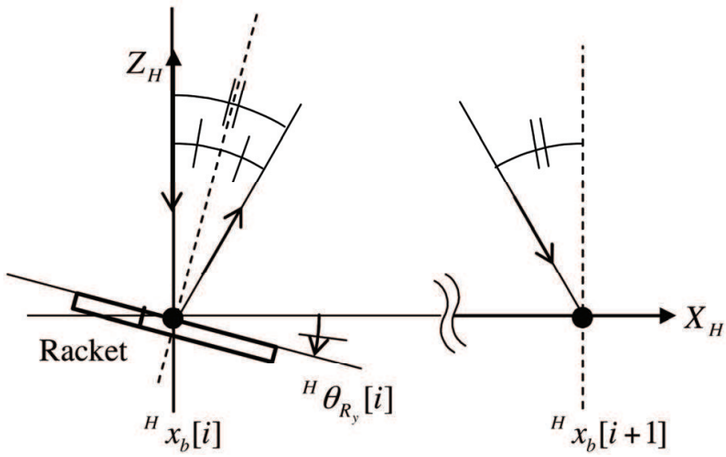

(b) x coordinate of Ball

Figure 10. The ball state transition Due to the hitting

$$ {}^H y_b[i+1] = {}^H y_b[i] - \frac{v_{b_0}^2 \sin 2{}^H\theta'_b[i]}{g} \tag{16} $$

$$ {}^H\theta_b[i+1] = -{}^H\theta'_b[i], \tag{17} $$

where v_{b_0} is the magnitude of the velocity of the ball just before the hit and

$$ {}^H\theta'_b[i] = -{}^H\theta_b[i] + 2{}^H\theta_{R_x}[i] \tag{18} $$

is the reflection angle of the ball after the hit. Since the initial ${}^H\theta_b[0] = 0$ from the control purpose and the desired value ${}^H\theta_{b_d} = 0$, the reflection angle ${}^H\theta'_b[i]$ can be small enough to assume that $\cos {}^H\theta'_b[i] \simeq 1$ and $\sin {}^H\theta'_b[i] \simeq \theta'_b[i]$. Due to this approximation, we get the linear discrete transition equation of the ball given by

$$\begin{bmatrix} {}^{H}x_b \\ {}^{H}y_b \\ {}^{H}\theta_b \end{bmatrix}[i+1] = \begin{bmatrix} 1 & 0 & 0 \\ 0 & 1 & \frac{2v_{b_0}^2}{g} \\ 0 & 0 & 1 \end{bmatrix} \begin{bmatrix} {}^{H}x_b \\ {}^{H}y_b \\ {}^{H}\theta_b \end{bmatrix}[i] + \begin{bmatrix} 0 & \frac{4v_{b_0}^2}{g} \\ -\frac{4v_{b_0}^2}{g} & 0 \\ -2 & 0 \end{bmatrix} \begin{bmatrix} {}^{H}\theta_{R_x} \\ {}^{H}\theta_{R_y} \end{bmatrix}[i]. \tag{19}$$

Note that the sampling times between the states $[i]$ and $[i + 1]$ (i = 0,1,2, ...) do not equal to each other. From the transition equation (19), the controllers for ${}^{H}\theta_{R_x}[i]$ and ${}^{H}\theta_{R_y}[i]$ to stabilize $({}^{H}x_b[i], {}^{H}y_b[i], {}^{H}\theta_b[i])$ are easily derived as

$$\begin{cases} {}^{H}\theta_{R_x}[i] = -k_{py}({}^{H}y_b[i] - {}^{H}y_{b_d}[i]) - k_\theta {}^{H}\theta_b[i] \\ {}^{H}\theta_{R_y}[i] = -k_{px}({}^{H}x_b[i] - {}^{H}x_{b_d}[i]) \end{cases}, \tag{20}$$

where ${}^{H}x_{b_d}[i]$ and ${}^{H}y_{b_d}[i]$ are the desired values expressed in $\Sigma_H[i]$, and k_{px},k_{py} and $k_\theta > 0$ are the control gains to be determined such that the eigenvalues of the closed system is smaller thanl. Note that it is impossible to get ${}^{H}x_b[i]$, ${}^{H}y_b[i]$, ${}^{H}\theta_b[i]$, ${}^{H}x_{b_d}[i]$ and ${}^{H}y_{b_d}[i]$ because these variables are the states of the ball at the hitting. Therefore, we have to use a prediction for these variables as the following section.

5.4 Prediction of Ball State

As mentioned in Section 5.3, from (20), we need the ball velocity just before the ith hit $v_{bx}[i]$, $v_{by}[i]$ and $v_{bz}[i]$ to calculate the incident angle ${}^{H}\theta_b[i]$. In this subsection, a simple prediction method of these variables is proposed.

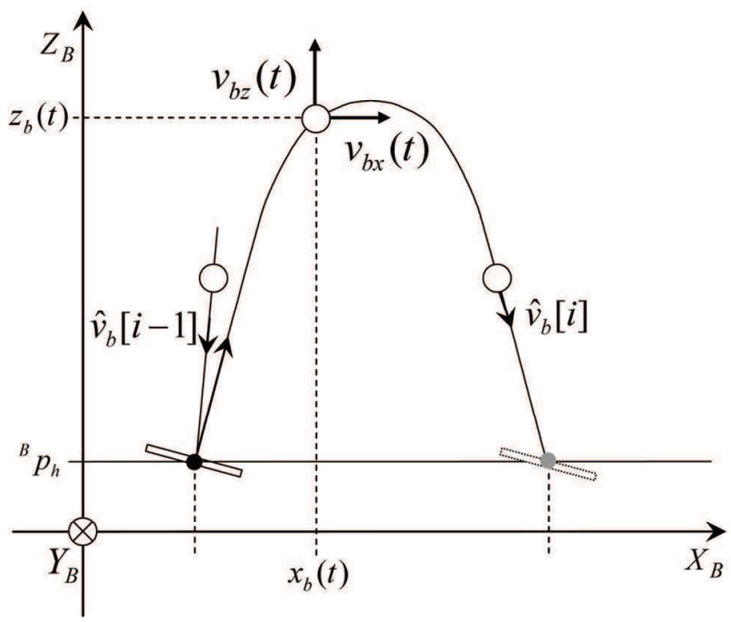

Figure 11. Prediction of Ball State

As shown in Fig. 11, ($x_b(t)$, $y_b(t)$, $z_b(t)$) are the ball position and ($v_{bx}(t)$,$v_{by}(t)$,$v_{bz}(t)$) are the ball velocity at time t between the $i-1$th and ith hits. $y_{bx}(t)$ and $v_{by}(t)$ are omitted for simplicity. Suppose the position and velocity of the ball can be detected by the visual sensor. From Assumption 1, the velocity ($v_{bx}[i]$, $v_{by}[i]$) at the ith hit are the same as ($v_{bx}(t)$,$v_{bz}(t)$). For the velocity $\hat{v}_{bz}[i]$, the predicted z velocity $v_{bz}[i]$ can be obtained from $v_{bz}(t)$ and $z_b(t)$ before the ith hit based on the energy conservation law:

$$\hat{v}_{bz}[i] = \sqrt{g(z_b(t) - p_h) + v_{bz}^2(t)}. \tag{21}$$

From this predicted velocity $\hat{v}_{bz}[i]$, the incident angle ${}^H\theta_b[i]$ is calculated as

$${}^H\hat{\theta}_b[i] = \tan^{-1}\frac{\sqrt{v_{bx}^2[i] + v_{by}^2[i]}}{v_{bz}[i]}. \tag{22}$$

Note that it is sufficient to replace ${}^Hx_b[i]$ and ${}^Hy_b[i]$ to ${}^Hx_b(t)$ and ${}^Hy_b(t)$ in the racket angle controller (20) because ${}^Hx_b(t)$ and ${}^Hy_b(t)$ equal ${}^Hx_b[i]$ and ${}^Hy_b[i]$ when the racket hits the ball. Therefore, it is not necessary to predict ${}^Hx_b[i]$ and ${}^Hy_b[i]$.

6. Experimental Result

The effectiveness of the proposed method is shown by a experimental result. In the control design, we need the variables ${}^Hx_b[i]$, ${}^Hy_b[i]$, ${}^H\theta_b[i]$, ${}^Hx_{b_d}[i]$ and ${}^Hy_{b_d}[i]$, which are calculated by the position and the velocity of the ball at the hit. As for a simple prediction of these variables, we use the position and velocity of the ball being the height 0.015[m] from the hitting horizontal plane as those of the ball at the hitting. The initial state of the robot manipulator is set such that the racket is horizontal as shown in Fig. 4. The initial position of the ball is above the racket. The desired value of the hitting position is set to ${}^B\boldsymbol{p}_H$ = [0.35 −0.65 0.35]^T [m]. The control gains are set to $k_{p_x} = k_{p_y} = 20 \times \frac{\pi}{180}$ [rad/m] and k_θ = 1.25. The control gain k_h effecting on the ball height is set to

$$k_h = \begin{cases} 0.275 & (E_b \le \bar{E}_b) \\ 0.275 - \frac{0.75}{g}(E_b - \bar{E}_b) & (E_b > \bar{E}_b) \end{cases},$$

where

$$E_b := ({}^Bp_{b_z} - {}^Bp_h)g + \frac{1}{2}\|{}^B\boldsymbol{p}_b\|^2, \quad \bar{E}_b := {}^B\bar{p}_{br}g.$$

E_b, is the total energy of the unit mass of the ball and ${}^B\bar{p}_{br}$ is the threshold value for the ball height. In this experiment, ${}^B\bar{p}_{br}$ is set to ${}^B\bar{p}_{br}$ = 0.070 [m].

The time interval to make the experiment is set to 100[s]. The experimental result is shown in Fig. 12. The left figure shows the trajectories of the ball and racket positions in the time interval 0-20[s]. The solid and the dashed trajectories represent the ball and the racket respectively. The solid horizontal lines are the desired hitting value. We can confirm that the x and y coordinates of the racket follow those of the ball and the z coordinate of the racket is symmetric to the ball with respect to the horizontal surface ${}^Bp_h$ = 0.35[m]. This result shows the effectiveness of the juggling preservation by controlling the racket position. On the other hand, the right figure shows the ball trajectory in the (x,y) plane. The white circle is the initial position and the black

circle is the desired hitting point. The big circle having the radius 0.05[m] is depicted with the center begin the desired hitting position. We can confirm that the most of the ball trajectory is included in the small circle. This result shows the effectiveness of the ball regulation problem by controlling the racket orientation. However, the average x and y positions have the errors 1.4[cm] and 3.6[cm] from the desired hitting position. As for this reason, the calculation errors and the uncertainty of the robot model can effect on the errors of the hitting position. On the other hand, the spread of the ball can be caused by the air resistance.

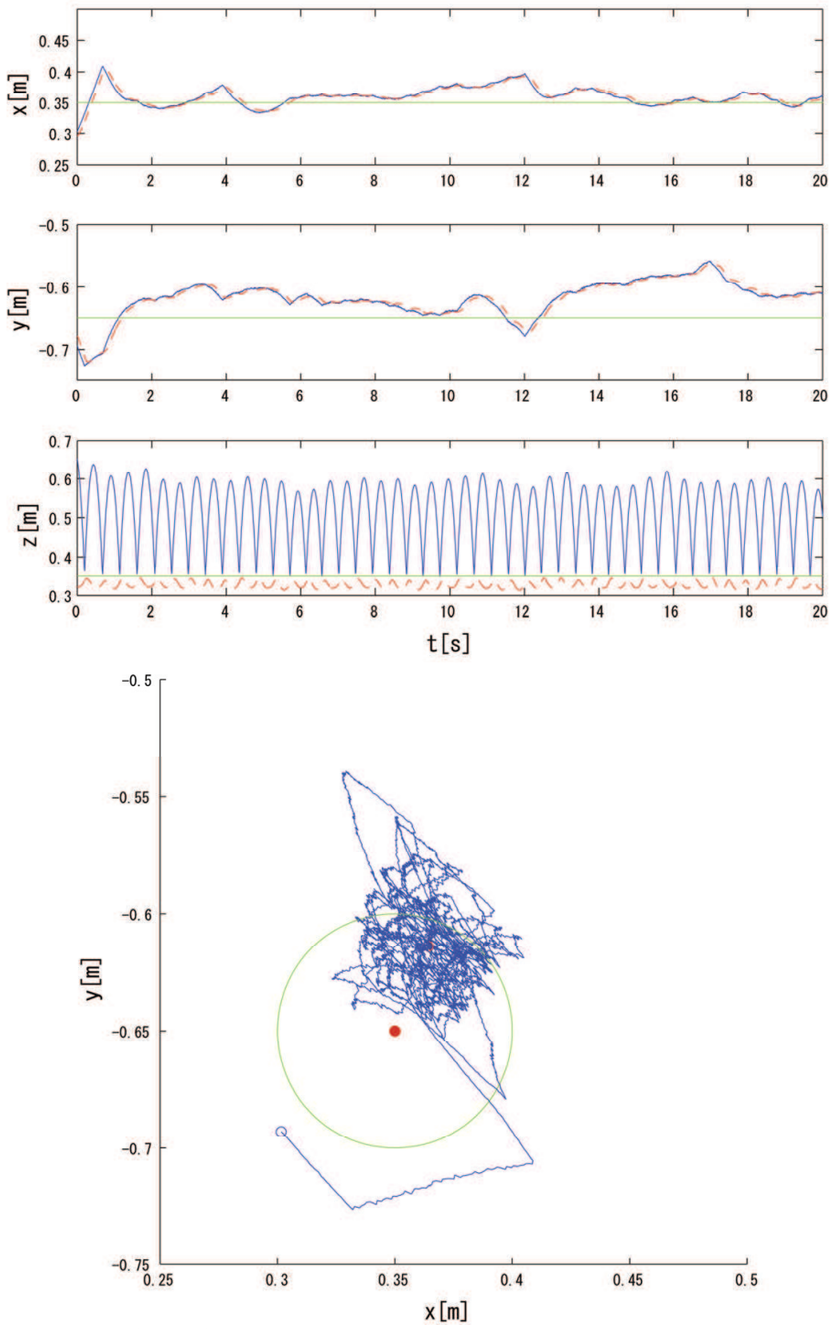

Figure 12. Experimental result

Next, the experiment with the disturbances for the ball is shown in Fig 13. The conditions for this experiment are same of the previous experiment. Not that the left figure is depicted in the time interval 0-100[s]. As for the disturbances, the ball was picked at random by a stick. We can confirm that the racket follows the ball and the ball juggling is preserved. This result shows the effectiveness of the juggling preservation problem and the robustness of the method. Readers can see the movie to represent the robustness in the website (Nakashima).

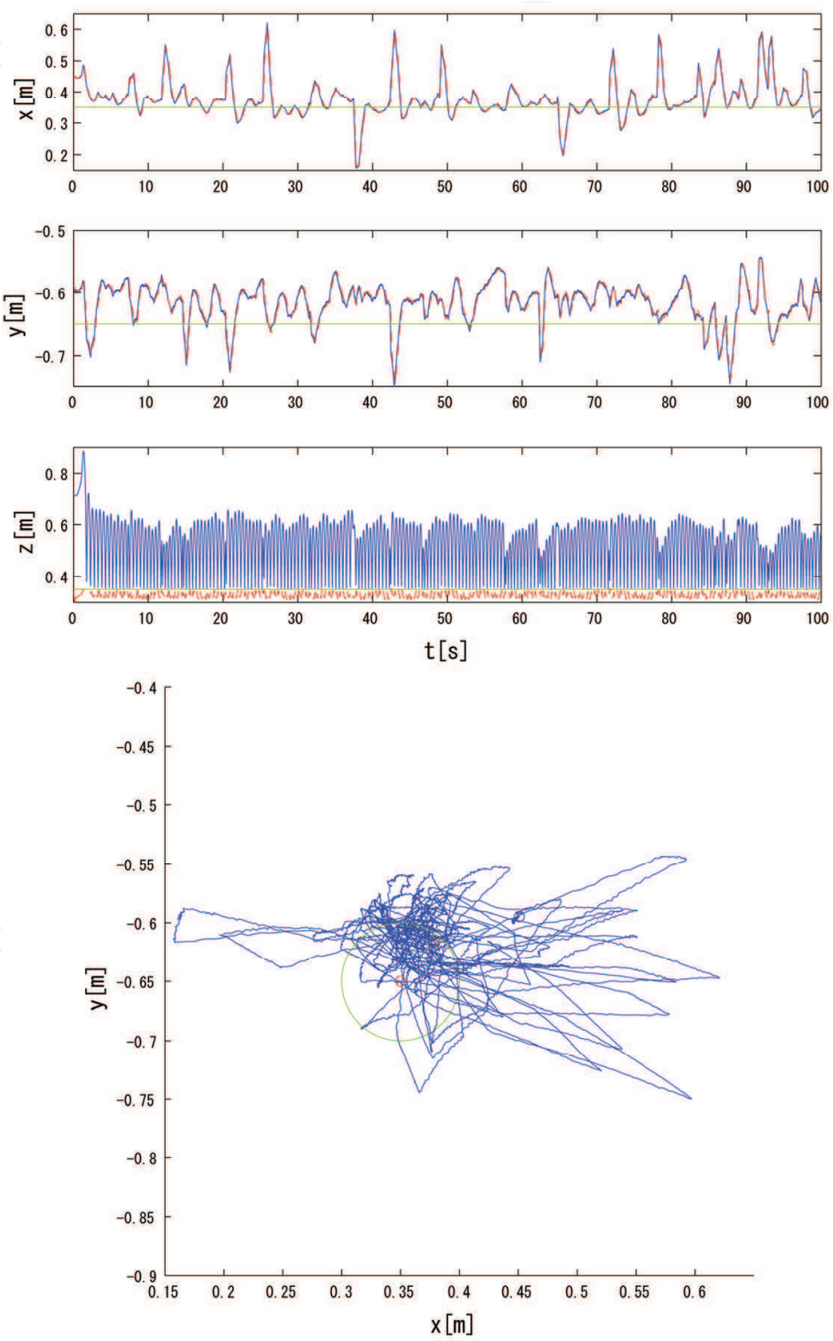

Figure 13. Experimental result with the disturbances for the ball

7. Conclusion

We realized the paddle juggling by a robot manipulator in this research. The key points are the following:

1. The method can hit the ball iteratively without the prediction of the fall point of the ball.
2. The method regulate the hitting position based on the ball state with the only prediction of the velocity in the z direction.

An example of another approach to the paddle juggling is to determine the racket position, angle and velocity based on the predicted ball trajectory in real time. This approach may be available while this needs more information about the ball than our proposed method. On the other hand, our method always tracks the ball in (x,y) plane and predicts only the z velocity. This contributes on the simplicity and the robustness. Furthermore, our method realizes the hitting with only synchronizing the ball in z direction. This contributes on no determination of the racket velocity for hitting the ball. To sum up, the simplicity and synchronous are significant to realize the paddle juggling. We hope that this may indicate that human do juggling based on the same strategy.

8. References

B. K. Ghosh, N. Xi, and T. J. Tarn. 1999. Control in Robotics and Automation: Sensor-Based Integration. Academic Press.

Buehler, M., D. E. Koditschek, and P. J. Kindlmann. 1994. Planning and Control of Robotic Juggling and Catching Tasks. *Int. J. Robot. Res*. 13 (2): 101-118.

Majima, S., and K. Chou. 2005. A Receding Horizon Control for Lifting Ping-Pong Ball. *IFAC World Congress*. Th-A04-TP/3.

Nakashima, A. http://www.haya.nuem.nagoya-u.ac.jp/~akira/data65s.wmv.

R. Mori, K. Hashimoto, E Takagi, and E Miyazaki. 2005. Examination of Ball Lifting Task using a Mobile Robot. *Proc. IEEE/RSJ Inter. Conf. Int. Robot. Sys*. 369-374.

Schaal, S., and C. G. Atkeson. 1993. Open Loop Control Strategies for Robot Juggling. *Proc. IEEE Inter. Conf. on Robot. Automat*. 913-918.

Robot Manipulators

Edited by Marco Ceccarelli

ISBN 978-953-7619-06-0

Hard cover, 546 pages

Publisher InTech

Published online 01, September, 2008

Published in print edition September, 2008

In this book we have grouped contributions in 28 chapters from several authors all around the world on the several aspects and challenges of research and applications of robots with the aim to show the recent advances and problems that still need to be considered for future improvements of robot success in worldwide frames. Each chapter addresses a specific area of modeling, design, and application of robots but with an eye to give an integrated view of what make a robot a unique modern system for many different uses and future potential applications. Main attention has been focused on design issues as thought challenging for improving capabilities and further possibilities of robots for new and old applications, as seen from today technologies and research programs. Thus, great attention has been addressed to control aspects that are strongly evolving also as function of the improvements in robot modeling, sensors, servo-power systems, and informatics. But even other aspects are considered as of fundamental challenge both in design and use of robots with improved performance and capabilities, like for example kinematic design, dynamics, vision integration.

InTech Europe
University Campus STeP Ri
Slavka Krautzeka 83/A
51000 Rijeka, Croatia
Phone: +385 (51) 770 447
Fax: +385 (51) 686 166
www.intechopen.com

InTech China
Unit 405, Office Block, Hotel Equatorial Shanghai
No.65, Yan An Road (West), Shanghai, 200040, China
中国上海市延安西路65号上海国际贵都大饭店办公楼405单元
Phone: +86-21-62489820
Fax: +86-21-62489821

IntechOpen